Folding Is Not Required for Bilayer Insertion: Replica Exchange Simulations of an α-Helical Peptide with an Explicit Lipid Bilayer

Hugh Nymeyer,[1] Thomas B. Woolf,[2] and Angel E. Garcia[1]*
[1]*Theoretical Biology & Biophysics Group, Los Alamos National Laboratory, Los Alamos, New Mexico 87545*
[2]*Departments of Physiology and of Biophysics, Johns Hopkins University, School of Medicine, Baltimore, Maryland 21205*

ABSTRACT **We implement the replica exchange molecular dynamics algorithm to study the interactions of a model peptide (WALP-16) with an explicitly represented DPPC membrane bilayer. We observe the spontaneous, unbiased insertion of WALP-16 into the DPPC bilayer and its folding into an α-helix with a transbilayer orientation. The free energy surface suggests that the insertion of the peptide into the DPPC bilayer precedes secondary structure formation. Although the peptide has some propensity to form a partially helical structure in the interfacial region of the DPPC/water system, this state is not a productive intermediate but rather an off-pathway trap for WALP-16 insertion. Equilibrium simulations show that the observed insertion/folding pathway mirrors the potential of mean force (PMF). Calculation of the enthalpic and entropic contributions to this PMF show that the surface bound conformation of WALP-16 is significantly lower in energy than other conformations, and that the insertion of WALP-16 into the bilayer without regular secondary structure is enthalpically unfavorable by 5–10 kcal/mol/residue. The observed insertion/folding pathway disagrees with the dominant conceptual model,[1–3] which is that a surface-bound helix is an obligatory intermediate for the insertion of α-helical peptides into lipid bilayers. In our simulations, the observed insertion/folding pathway is favored because of a large (>100 kcal/mol) increase in system entropy that occurs when the unstructured WALP-16 peptide enters the lipid bilayer interior. The insertion/folding pathway that is lowest in free energy depends sensitively on the near cancellation of large enthalpic and entropic terms. This suggests the possibility that intrinsic membrane peptides may have a diversity of insertion/folding behaviors depending on the exact system of peptide and lipid under consideration. Proteins 2005;59:783–790.**

Key words: four-stage model; replica exchange molecular dynamics; WALP

INTRODUCTION

Membranes and membrane proteins are dynamically active systems involved in essential biological processes. Whole genome analysis indicates that 20–30% of all open reading frames code for membrane spanning α-helical bundle proteins.[4,5] Proteins with β-barrel architectures (e.g., porins) are coded for by several percent of the open reading frames in bacteria[6] and an unknown fraction in eukaryotic organisms. Many other proteins involved in cell–cell adhesion, immune recognition, and signal transduction also have single α-helical membrane spanning domains.[7] Because of difficulties in isolating, purifying, and crystallizing membrane proteins, only about 82 unique intrinsic membrane protein structures are known[3,8] at atomic resolution compared with the thousands of globular proteins that have been solved.[9] Consequently, the protein–protein and protein–lipid interactions that stabilize intrinsic membrane proteins are not as well understood as the interactions that stabilize globular proteins. Prediction of membrane protein structure, of membrane protein folding, and of membrane protein dynamics is limited by our understanding of these protein–lipid interactions and lipid dynamics.[10]

Because of these difficulties, model systems have been instrumental for understanding the general principles governing membrane protein structure and dynamics. An important model system has been the WALP series of peptides, which have an alternating, variable length alanine/leucine core flanked on both termini by two tryptophan residues.[11–13] These peptides have been demonstrated to form transmembrane α-helices by CD,[11] NMR,[11,14,15] UV-Vis spectroscopy,[14] transmission and atomic force microscopy,[16,17] and mass spectrometry.[18–20] The compensatory changes in lipid structure induced by WALP peptides have also been studied via NMR,[11,20–26] electron spin resonance,[21,22] microscopy,[24] X-ray diffraction,[27] and calorimetry.[25] These experimental studies have been complemented by molecular dynamics calculations, which have attempted to discern what lipid and peptide structural adjustments might occur for different length WALPs and different bilayer settings.[28]

Grant sponsor: the US DOE by LDRD project.

*Correspondence to: Angel Garcia, Theoretical Biology & Biophysics Group, T-10, MS K710, T-10, Los Alamos National Laboratory, Los Alamos, NM 87545. E-mail: angel@rpi.edu

Received 29 October 2004; Accepted 23 November 2004

Published online 12 April 2005 in Wiley InterScience (www.interscience.wiley.com). DOI: 10.1002/prot.20460

In this article we report all-atom simulations of the interactions of a 16-residue WALP peptide with a solvated DPPC bilayer. Our simulations show the spontaneous insertion and folding of this WALP-16 peptide into the DPPC bilayer. These simulations are the first to show the unbiased spontaneous insertion and folding of a hydrophobic peptide into an explicitly represented lipid bilayer. The spontaneous insertion and folding of peptides into transbilayer configurations is difficult to observe, because most membrane spanning peptides are highly hydrophobic and thus prone to aggregation. To our knowledge, only three experimental kinetic studies of spontaneous peptide insertion processes exist.[29–31] Although no kinetic measurements of WALP insertion have been made, generic models of peptide insertion and folding have been constructed based on thermodynamic arguments.[1–3] Our simulated insertion does not agree with these models, suggesting that other previously discounted thermodynamic effects in the lipid component may alter the insertion process in some peptide/bilayer systems.

Our simulations have been conducted using 1024 processors on the Q-machine, a parallel computer at Los Alamos National Laboratory, which, at the time of this simulation, was ranked as the third fastest in the world.[32] We have implemented a replica exchange (parallel tempering) molecular dynamics algorithm[33] on this machine. Replica exchange algorithms[33–37] were developed to study glassy systems with long relaxation times and are widely used in the context of protein folding[38–40] (reviewed by Nymeyer et al.[41]). In these methods, multiple copies or replicas of the same system are simulated in parallel at different temperatures, and temperatures are periodically exchanged between two replicas in a manner that preserves detailed balance. These algorithms speed equilibration by a large factor (perhaps 100x or more)[42–44] and enable us to observe insertion of a WALP peptide while simultaneously computing the equilibrium properties of the WALP/DPPC bilayer system.

As described in the Methods section, we run three simulations. The first simulation begins with the peptide in a water solvated conformation. This simulation shows WALP spontaneously moving into conformations in which it is anchored into the bilayer. The second simulation starts with the peptide in an anchored conformation. This simulation shows four separate events in which WALP spontaneously inserts completely into the bilayer and forms an α-helical secondary structure. The third simulation, which begins with the peptide inserted completely in the bilayer, is used to generate an equilibrium ensemble of WALP/DPPC conformations and measure the changes in thermodynamic quantities as a function of peptide structure and location in the bilayer.

The first two simulations suggest an insertion mechanism for WALP with three steps. In the first step, the peptides move into a membrane-anchored conformation. In this conformation, the peptide has inserted one or more of its Trp residues into the bilayer below the phosphate groups. These Trp residues anchor the peptide to the bilayer, although the peptide itself is still mostly water solvated. In the second step, the peptides insert into the lipid bilayer in an unstructured state, occupying the volume exposed in the lipid due to fluctuations of the lipid chains. In the third step, these peptides form a helical nucleus, from which the whole α-helix rapidly forms. This helix orients roughly normal to the bilayer surface. These basic steps are observed in all the WALP peptides that inserted and folded. No WALPs were observed to insert directly from a surface-bound helical conformation.

One of the observed insertion trajectories is shown in Figure 1. Steps in the trajectory are shown along with a projection of the trajectory onto the plane spanned by distance of the WALP from the central bilayer plane and helical content of the WALP peptide. This trajectory is superimposed upon the potential of mean force (PMF). The trajectory of the inserted peptides mirrors the underlying potential of mean force determined in equilibrium.

The PMF at this temperature has three dominant basins of attraction. In the first basin, the peptide is mostly water solvated and nonhelical but possibly anchored via one or more Trp residues into the membrane. In the second basin, the peptide is located in the bilayer interface and nonhelical. This basin is an ensemble of states in which the peptide is lying approximately in the plane of the interface and states in which the peptide is approximately normal to the interface. In the third basin, the peptide is helical and inserted in the membrane. The principal barrier to folding occurs during nucleation of the peptide in the center of the lipid bilayer. Although our PMF is shown for temperatures greater than the experimental conditions, extrapolation to lower temperatures does not appear to alter the insertion mechanism; however, the barrier to insertion does increase with decreasing temperature.

By fitting the temperature variation of our PMF, we have estimated the enthalpic and entropic changes of our system with peptide structure and position. These results (Fig. 2) agree with the known thermodynamics of peptides interacting with lipid bilayer. In particular, we find that the insertion of the WALP-16 peptide into the DPPC bilayer in a largely unstructured state entails a significant enthalpic penalty of between 5–10 kcal/mol per residue. This is in agreement with calculations[45] and measurements on model compounds[46,47] that provide estimates of an enthalpic backbone desolvation penalty of 6–8 kcal/mol per residue. As expected, the enthalpy decreases sharply by nearly the same amount with the growth of hydrogen bonds along the α-helix. Although helix formation in water is generally enthalpically favored, helix formation followed by insertion may be less enthalpically favorable or even unfavorable, because hydrogen bonds in a fully formed α-helix retain some residual electrostatic interaction with the surrounding solvent.[48] Our calculations, however, disagree with the prevailing four-stage model in which peptide folding occurs before insertion (Fig. 3), and suggest that for WALP insertion may occur before folding.

Waters bound to the WALP may play an important role in stabilizing the peptide when inserted in the bilayer. Although we have prevented waters from penetrating to the center of the bilayer via a weak mean-field potential

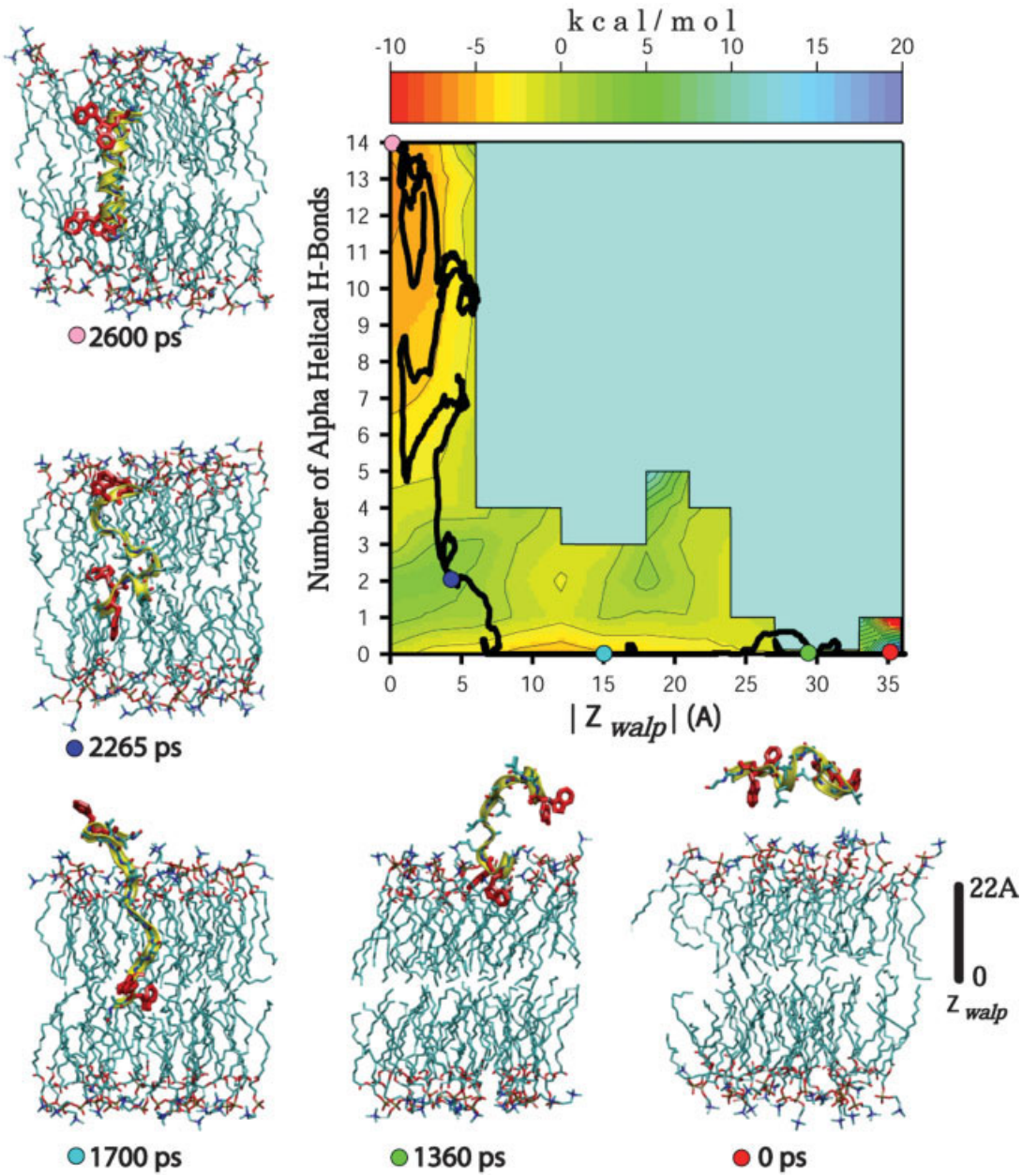

Fig. 1. A folding trajectory for the WALP-16 is shown projected onto a two-dimensional surface. The surface shows, with color and contour lines, the relative free energy changes along the changes in hydrogen bonding of the helix and the *z*-position of the center of mass of the peptide relative to the bilayer center. Color changes occur at 1-kcal/mol intervals; solid contour lines are drawn at 2-kcal/mol intervals. All folding trajectories followed a similar route with initial stabilization of Trp at the interface followed by insertion and then folding.

(see Methods for details), we still observe a significant amount of water bound to the WALP backbone prior to α-helix formation (see Fig. 4). Bound waters are certain to make insertion of the unfolded peptide more favorable than would be expected based on complete backbone desolvation. The two curves in Figure 4(a) were produced by combining the data at many different temperatures. This data was combined by first sorting the electrostatic interaction energy by temperature. At each temperature, the electrostatic energy versus position data was binned into overlapping bins of 5-Å width. The average electrostatic energy in each bin was assumed to have a linear variation with temperature. A least-squares fit of energy versus temperature was used to determine the best estimate for the average electrostatic energy in each bin at 450 K. Any temperature with fewer than 10 sampled energies in a bin was not included in the linear fit. The same procedure was followed to compute the number of bound waters versus position. The vertical bars show estimated maximum errors. Figure 4(b) shows a configuration of the

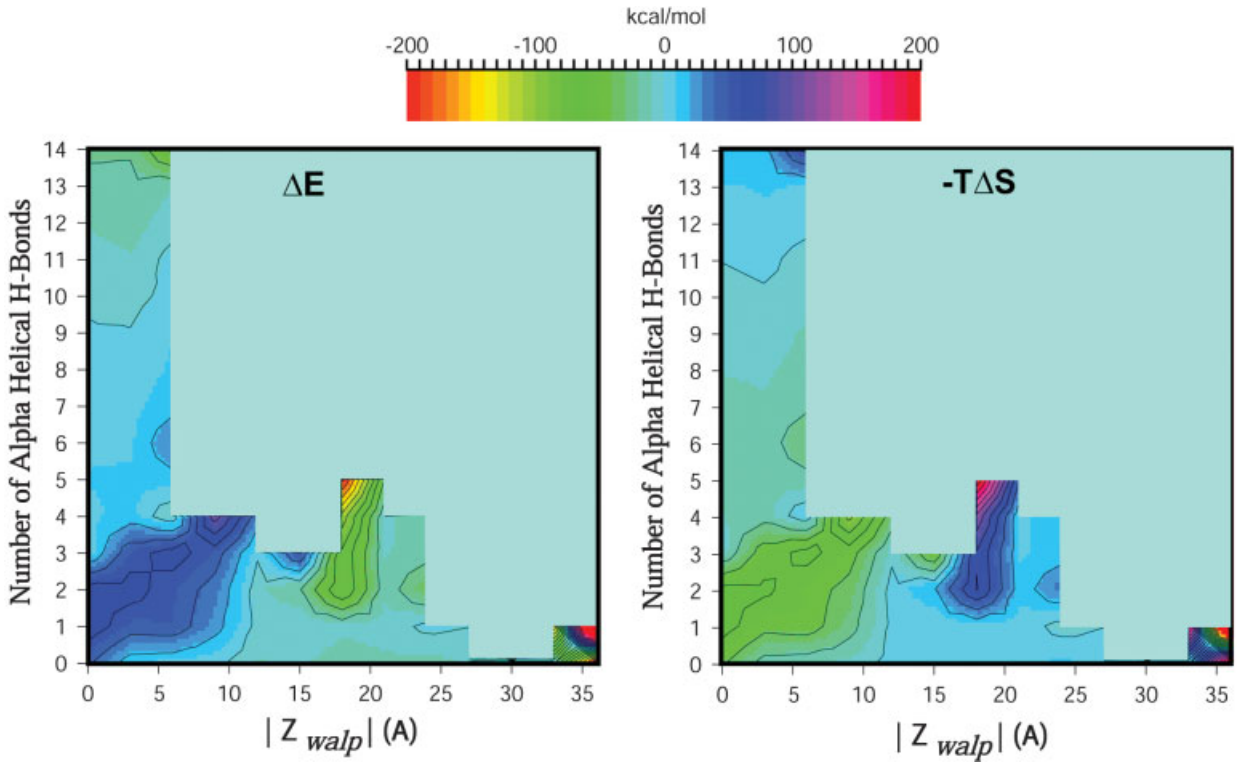

Fig. 2. Relative changes in enthalpy and entropy show the trade-offs that occur with peptide binding and insertion during the folding process. Colors change at 10-kcal/mol intervals; solid contour lines are drawn at 20-kcal/mol intervals. In particular, note the gain in enthalpic energy due to initial binding and the 7–11-kcal/mol gain in enthalpy due to hydrogen bond formation during the α-helical folding within the bilayer interior.

inserted peptide and water molecules within the lipid/water interface near the peptide.

Figure 2 indicates that, initially, insertion of the WALP is not strongly disfavored by enthalpy, presumably due to the presence of these bound waters. From Figure 2 we see that the surface bound partly helical conformations of the peptide are exceptionally low in energy. There are few experimental measurements of enthalpy changes upon the binding of small molecules to lipid bilayers. Jacobs and White[2] found negligible enthalpy changes upon binding of the small peptides Ala-X-Ala-O-*tert*-butyl (X = Leu, Phe, Trp) to DMPC vesicles. Similar results were found the COX IV peptide[49] and for several Trp derivatives.[50] In contrast, many aromatic amphiphiles have negative enthalpy changes upon binding to lipid bilayers.[3,51–53] DeVido et al.[54] suggest that negative enthalpic changes are generic for spontaneous binding of small molecules to ordered lipid chain phases. Figure 5 indicates that a strong Coulombic interaction can exist between the TRP residues that cap WALP and the phosphatidylcholine groups. This strong interaction is consistent with the experiments and statistical studies[55] that suggest favorable enthalpic interactions between Trp side chains and the DPPC/water interface. It is also expected that α-helical hydrogen bonds will be more enthalpically favorable in the interface, because its effective dielectric constant is reduced from that of bulk water (probably to an ε of ≈18).[3,56,57]

Although the partially folded helical surface bound conformations of WALP are low in energy, no passage of these conformations to a transmembrane helix is observed, suggesting that the surface bound state is acting more as an off-pathway trap than an intermediate for WALP insertion. Peptides other than WALP may be more stabilized as interfacial helices. Stronger stabilization of interfacial helices should favor insertion directly from a surface bound helical conformation.

The observed insertion behavior and the equilibrium potential of mean force disagree with the prevailing hypothesis about the spontaneous insertion of peptides into lipid bilayers.[1–3] The accepted hypothesis, known as the four-stage model (Fig. 3), posits that insertion into the membrane interior should occur only after significant secondary structure has already formed. This conclusion is based on calculations[45] and measurements[46,47] using bulk hydrophobic solvents, which show that the insertion of an unstructured peptide into the lipid interior will entail a high enthalpic cost due to the desolvation of the peptide backbone. This desolvation penalty is mostly absent in regularly structured peptides, because the backbone is already desolvated to a large extent, and the peptide hydrogen bond donors and acceptors are satisfied internally.

Our simulations are in agreement with the calculations and measurements suggesting a large energetic penalty for backbone desolvation. However, our simulations also show that entropic changes are strong enough to overcome this desolvation penalty. No reliable estimates or measurements of the entropic changes due to the insertion of an

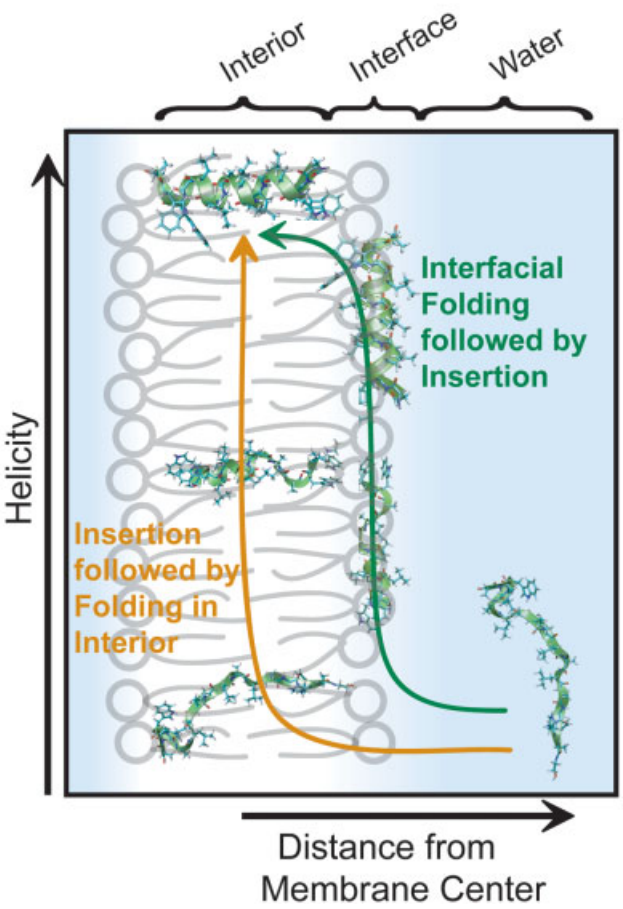

Fig. 3. The prevailing conceptual model of helical peptide insertion postulates that all transmembrane domains will fold within the interfacial zone and then insert as a folded domain into the bilayer. The simulation results suggest, at least for this peptide, that the alternative pathway of partial binding at the interface, insertion to the bilayer interior and then folding to an α-helix can be the preferred route for folding.

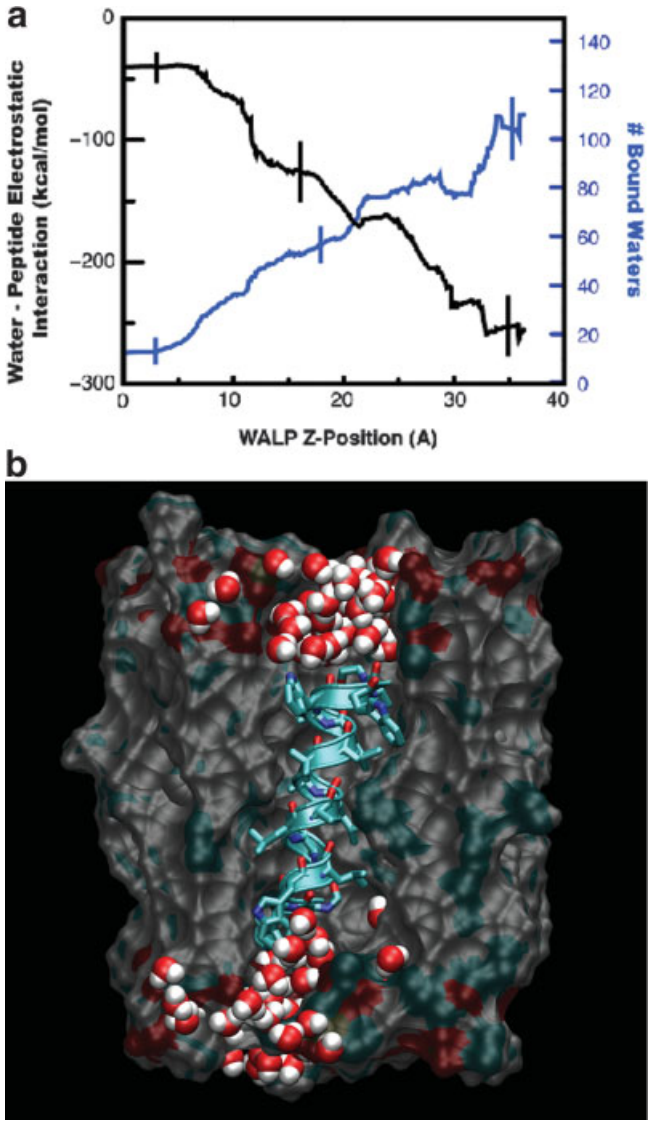

Fig. 4. (**a**) The electrostatic interaction energy between WALP and water as a function of WALP center of mass distance from the bilayer central plane (black). Also shown is the number of bound waters versus position (blue) determined by counting all waters with an oxygen atom less than 4.0 Å in distance from any peptide atom. The bilayer central plane is positioned at $z = 0$ Å, and the water–lipid interface is near $z = 20$ Å. Even when the peptide is inserted deep into the membrane; it retains a significant interaction with the aqueous solvent, mostly through the existence of bound waters; consequently, it is not correct to think of the peptide as being completely desolvated even when it is in the center of the bilayer. (**b**) Illustration of a typical configuration of the alpha helical peptide inside the lipid bilayer and interacting with waters at the lipid/water interface.

unstructured peptide into a lipid bilayer exist to which we may compare our simulations; however, the observed entropic compensation effect is too large to be purely a simulation artifact.

Our molecular dynamics simulation results depend significantly on the force field used for the protein and the lipid and on the simulation conditions such as constant volume, constant cross-sectional surface area, and system size. For example, we observe a transition to an ordered, gel-like tilted phase for the lipid below 400 K, while the transition should occur at 314 K. However, our simulations provide a molecular view of the folding of a transmembrane α-helix within an explicit lipid bilayer and suggest that the insertion and folding of peptides into lipid bilayers might be more complex than suggested. Simulations of peptides that are known to coexist in the water and lipid phases[58,59] are under way. We expect our simulations to motivate experimentation of the time resolved kinetics of the insertion and folding of peptides in membranes.

In conclusion, our simulations provide a molecular view of the folding of a transmembrane α-helix within an explicit lipid bilayer. Our results show that the folding process might be more complex and subtle than suggested by the four-stage model. In particular, we observe large entropic changes in the system that may make insertion of peptides into the bilayer prior to secondary structure formation favorable. The composition of the peptide and lipid are certain to modulate the large enthalpic and entropic terms driving insertion, making insertion mechanisms more variable than have been suggested by the four-stage model. In this regard we suggest that mem-

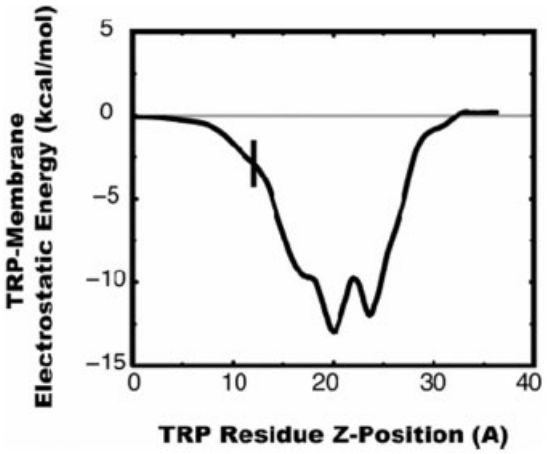

Fig. 5. The Coulomb interaction energy between the TRP residues and the bilayer as a function of their center of mass positions. The bilayer central plane is positioned at $z = 0$, and the water–lipid interface is near $z = 20$ Å. The TRP residues have a strong electrostatic interaction with the lipid phosphatidylcholine groups that works to stabilize conformations with TRP in this region. The electrostatic interaction energy between TRP and the membrane showed only a small temperature dependence, so all temperature data was combined and binned using a 2-Å bin width. The vertical bar is an estimated maximum error.

brane proteins, like globular proteins, may have multiple folding routes best described as motion on a multidimensional free energy surface.[60,61] More experimental studies of the folding pathways for α-helical monomers and dimers would be useful to further understand the molecular interplay that occur within the heterogenous solvation setting of the membrane bilayer and its associated waters.

METHODS

Initial Conditions

The starting point of our simulations is a fully solvated WALP-16 peptide [CHO-ALA-TRP_2-$(LEU\text{-}ALA)_5$-TRP_2-ALA-Ethanolamine] with 1048 TIP3P waters and a bilayer with 18 DPPC molecules in each monolayer. The initial conditions of the lipid were derived from previous simulations of the WALP-16 in a DPPC bilayer.[8] The WALP-16 peptide was placed initially into an unfolded water-solvated conformation with its long axis approximately horizontal to the membrane plane. The surface area per lipid in this initial conformation is 68 Å^2. The surface area per lipid in pure DPPC bilayers has been measured[62] to be 64 Å^2; however, the surface area for a mixed DPPC/WALP system is not accurately known. We assumed a constant surface area throughout the insertion process. This surface area was chosen to match the result of another DPPC/WALP simulation performed with the same force field.[28]

Simulations

Simulations were carried out via a modified version of the CHARMM (version 28) program.[63] The force field/energy function was the CHARMM22 all-atom force field of Schlenkrich et al.[64,65]

The initial simulation was a 1-ns replica exchange simulation using 38 replicas of the system with temperatures exponentially spaced from 350–505.8 K. This was followed by a 1.6-ns simulation involving 64 replicas exponentially spaced from 350 to 800 K, where the simulation continued from a membrane anchored conformation obtained at the end of the initial 1ns simulation. Our lowest temperature is above the experimentally known phase transition of the DPPC bilayer (~314 K).

For N replicas, exchanges are attempted between N^2 randomly chosen pairs of replicas at intervals of 250 integration steps. Integration steps are 2 fs for the first 1.4 ns; 0.8 fs for the next 200 ps; and 1 fs for the remainder. All bonds involving water are fixed for the first 1.6 ns; all bonds involving hydrogen are fixed for the last 1 ns. PME is used for the electrostatics with a $32 \times 32 \times 64$ grid with fourth order spline interpolation, a 4-Å width Gaussian screening charge, and a 10–12-Å switching function on the direct interaction. The ensemble is NVT in a $35 \times 35 \times 72.75$-Å box with a Nose-Hoover thermostat with a mass of 500 a.u.

A planar restraint is placed on the average position of the C_2 atom in each DPPC monolayer to maintain the membrane structure at high temperature. The minima are at $=18.3555$ Å and -18.2203 Å. The restraining potential is zero within 0.25 Å of the minimum and quadratic with a 10 kcal/mol/Å^2 force constant outside this region. A quadratic restraint of the form 0.2 kcal/mol-Å$^2 \times D^2 \times (D^2 - 2.25$ Å$^2)$ applies to the water oxygens where $D = z - 25$ Å for $z > 0$ and $D = z = 25$ Å for $z < 0$. The effect of these constraints on the equilibrium properties of the lipid appears to be minimal since the calculated surface area tension of 35 dyn/cm at low T is consistent with the values reported for the force field used in our calculations.[66] The calculated surface tension decreases as T increases and becomes negative at $T > 430$ K.

The equilibrium simulation has identical settings. All replicas are started inserted but are nonhelical. Step size is 0.8 fs for the first 200 ps with only the waters held rigid and 1 fs for the remainder with all bonds involving hydrogen held fixed. Total simulation time is 3.5 ns per replica. The final 1.5 ns is used for analysis.

Analysis

The potential of mean force was computed for each temperature as $-RT\ln(N)$, where N is the number of counts per bin at temperature T in Kelvin, and R is the ideal gas constant in units of kcal/mol/K. The abscissa is the absolute value of the Z-coordinate of the WALP-16 center of mass with origin placed at the bilayer center. The ordinate is the number of α-helical hydrogen bonds determined with a 3.5-Å cutoff on the hydrogen–oxygen distance and a 90° cutoff on the angle between the C–O and H–N vectors.

All points in the potential of mean force plane with counts at 7 or more temperatures were used to determine the thermodynamic formula:

$$\Delta G = \Delta E - T\Delta S$$

$$\Delta E = \Delta E_0 + \int_{T0}^{T} \Delta Cv dT'$$

$$\Delta S = \Delta S_0 + \int_{T0}^{T} \frac{\Delta Cv}{T'} dT'$$

$$\Delta Cv = \Delta Cv_0 + (d\Delta Cv/dT)_0(T - T_0)$$

where the four parameters are: relative energy ΔE_0 at temperature T_0, relative entropy ΔS_0, relative heat capacity ΔCv_0, and the change in relative heat capacity with temperature $(d\Delta Cv/dT)_0$. Contours of ΔG are shown in Figure 1. Contours of ΔE and $-T\Delta S$ are shown in Figure 2. Points sampled at fewer than seven temperatures are not shown.

ACKNOWLEDGMENTS

We thank A. Ladokhin, R.W. Pastor, and S.H. White for enlightening discussions. Computer facilities were provided by Los Alamos Institutional Computing. In particular, we thank D. Dawson, H. Marshall, M. Vigil, and C. Wampler for their assistance in porting code and using the Q machine at Los Alamos.

REFERENCES

1. Popot JL, Engelman, DM. Membrane-protein folding and oligomerization: the 2-stage model. Biochemistry 1990;29:4031–4037.
2. Jacobs RE, White SH. The nature of the hydrophobic binding of small peptides at the bilayer interface: implications for the insertion of transbilayer helices. Biochemistry 1989;28:3421–3437.
3. White SH, Wimley WC. Membrane protein folding and stability: physical principles. Annu Rev Biophys Biomol Struct 1999;28:319–365.
4. Boyd D, Schierle C, Beckwith J. How many membrane proteins are there? Protein Sci 1998;7:201–205.
5. Wallin E, Von Heijne G. Genome-wide analysis of integral membrane proteins from eubacterial, archaean, and eukaryotic organisms. Protein Sci 1998;7:1029–1038.
6. Wimley WC. Toward genomic identification of β-barrel membrane proteins: compositions and architecture of known structure. Protein Sci 2002;11:301–312.
7. Landoltmarticorena C, Williams KA, Deber CM, Reithmeier RAF. Nonrandom distribution of amino acids in the transmembrane segments of human type-I single span membrane-proteins. J Mol Biol 1993;229:602–608.
8. White S. Membrane proteins of known 3D structure. http://blanco.biomol.uci.edu/Membrane_Proteins_xtal.html. Accessed 2004 May 10.
9. Berman HM, Westbrook J, Feng Z, Gilliland G, Bhat TN, Weissig H, et al. The Protein Data Bank. Nucleic Acids Res 2000;28:235–242 (see also http://www.rcsb.org/pdb).
10. Popot JL, Engelman DM. Helical membrane protein folding, stability, and evolution. Annu Rev Biochem 2000;69:881–922.
11. Killian JA, et al. Induction of nonbilayer structure in diacylphosphatidylcholine model membranes by transmembrane α-helical peptides: importance of hydrophobic mismatch and proposed role of tryptophans. Biochemistry 1996;35:1037–1045.
12. Killian JA. Hydrophobic mismatch between proteins and lipids in membranes. Biochim Biophys Acta Rev Biomembr 1998;1376:401–416.
13. De Planque MRR, Killian JA. Protein–lipid interactions studied with designed transmembrane peptides: role of hydrophobic matching and interfacial anchoring (review). Mol Membr Biol 2003;20:271–284.
14. de Planque MRR, et al. Sensitivity of single membrane-spanning α-helical peptides to hydrophobic mismatch with a lipid bilayer: effects on backbone structure, orientation, and extent of membrane incorporation. Biochemistry 2001;40:5000–5010.
15. van der Wel PCA, et al. Geometry and intrinsic tilt of a tryptophan-anchored transmembrane α-helix determined by ^{2}H NMR. Biophys J 2002;83:1479–1488.
16. Rinia HA, et al. Visualization of highly ordered striated domains induced by transmembrane peptides in supported phosphatidylcholine bilayers. Biochemistry 200;39:5852–5858.
17. Rinia HA, et al. Domain formation in phosphatidylcholine bilayers containing transmembrane peptides: specific effects of flanking residues. Biochemistry 2002;41:2814–2824.
18. Demmers JAA, et al. Electrospray ionization Mass Spectrometry as a tool to analyze hydrogen/deuterium exchange kinetics of transmembrane peptides in lipid bilayers. Proc Natl Acad Sci USA 2000;97:3189–3194.
19. Demmers JAA, et al. Interfacial positioning and stability of transmembrane peptides in lipid bilayers studied by combining hydrogen/deuterium exchange and mass spectrometry. J Biol Chem 2001;276:34501–34508.
20. de Planque MRR, et al. Interfacial anchor properties of tryptophan residues in transmembrane peptides can dominate over hydrophobic matching effects in peptide–lipid interactions. Biochemistry 2003;42:5341–5348.
21. de Planque MRR, et al. Influence of lipid/peptide hydrophobic mismatch on the thickness of diacylphosphatidylcholine bilayers. a ^{2}H NMR and ESR study using designed transmembrane α-helical peptides and gramicidin A. Biochemistry 1998;37:9333–9345.
22. de Planque MRR, et al. Different membrane anchoring positions of tryptophan and lysine in synthetic transmembrane α-helical peptides. J Biol Chem 1999;274:20839–20846.
23. Morein S, et al. The effect of peptide/lipid hydrophobic mismatch on the phase behavior of model membranes mimicking the lipid composition in *Escherichia coli* membranes. Biophys J 2000;78:2475–2485.
24. de Planque MRR, et al. The effects of hydrophobic mismatch between phosphatidycholine bilayers and transmembrane α-helical peptides depend on the nature of interfacially exposed aromatic and charged residues. Biochemistry 2002;41:8396–8404.
25. Morein S, Killian JA, Sperotto MM. Characterization of the thermotropic behavior and lateral organization of lipid–peptide mixtures by a combined experimental and theoretical approach: effects of hydrophobic mismatch and role of flanking residues. Biophys J 2002;82:1405–1417.
26. Morein S, et al. Influence of membrane-spanning α-helical peptides on the phase behavior of the dioleoylphosphatidylcholine/water system. Biophys J 1997;73:3078–3088.
27. Weiss TM, et al. Hydrophobic mismatch between helices and lipid bilayers. Biophys J 2003;84:379–385.
28. Petrache HI, Zuckerman DM, Sachs JN, Killian JA, Koeppe RE, Woolf TB. Hydrophobic matching mechanism investigated by molecular dynamics simulations. Langmuir 2002;18:1340–1351.
29. Hunt JF, Rath P, Rothschild KJ, Engelman DM. Spontaneous, pH-dependent membrane insertion of a transbilayer α-helix. Biochemistry 1997;36:15177–15192.
30. Meijbert W, Booth PJ. The activation energy for insertion of transmembrane α-helices is dependent on membrane composition. J Mol Biol 2002;319:839–853.
31. Yano Y, Matsuzaki K. Membrane insertion and dissociation processes of a model transmembrane helix. Biochemistry 2002;41:12407–12413.
32. Dongarra JJ, Meuer HW, Strohmaier E. TOP500 supercomputer sites. Supercomputer 1997;13:89–120 (see also http://www.top500.org).
33. Sugita Y, Okamoto Y. Replica-exchange molecular dynamics method for protein folding. Chem Phys Lett 1999;314:141–151.
34. Swendsen R, Wang J. Replica Monte Carlo simulation of spinglasses. Phys Rev Lett 1986;57:2607–2609.
35. Marinari E, Parisi G. Simulated tempering—a new Monte-Carlo scheme. Europhys Lett 1992;19:451–458.
36. Geyer C, Thompson E. Annealing Markov-chain Monte-Carlo with applications to ancestral inference. J Am Stat Assoc 1995;90:909–920.
37. Hukushima K, Nemoto K. Exchange Monte-Carlo simulations and application to spin glass simulations. J Phys Soc Jpn 1996;65:1604–1608.
38. Hansmann, U. Parallel tempering algorithm for conformational

studies of biological molecules. Chem Phys Lett 1997;281:140–150.
39. Garcia AE, Sanbonmatsu KY. Exploring the energy landscape of a β hairpin in explicit solvent. Protein Struct Funct Genet 2001;42:345–354.
40. Sanbonmatsu KY, Garcia AE. Structure of met-enkephalin in explicit aqueous solutions using replica exchange molecular dynamics. Protein Struct Funct Genet 2002;46:225–234.
41. Nymeyer H, Gnanakaran S, Garcia AE. Atomic simulations of protein folding, using the replica exchange algorithm. Methods Enzymol 2004;383:119–149.
42. Garcia AE, Sanbonmatsu KY. Alpha-helical stabilization by side chain shielding of hydrogen bonds. Proc Natl Acad Sci USA 2002;99:2782–2787.
43. Yamamoto R, Kob W. Replica-exchange molecular dynamics simulation for supercooled liquids. Phys Rev E 2000;61:5473–5476.
44. Bedrow D, Smith GD. Exploration of conformational phase space in polymer melts: a comparison of parallel tempering and conventional molecular dynamics simulations. J Chem Phys 2001;115:1121–1124.
45. Ben-Tal N, Sitkoff D, Topol IA, Yang A-S, et al. Free energy of amide hydrogen bond formation in vacuum, in water, and in liquid alkane solution. J Phys Chem B 1997;101:450–457.
46. Roseman MA. Hydrophobicity of the peptide C═O · · · H—N hydrogen-bonded group. J Mol Biol 1998;201:621–623.
47. Wimley WC, Creamer TP, White SH. Solvation energies of amino acid side chains and backbone in a family of host–guest pentapeptides. Biochemistry 1996;35:5109–5124.
48. Ben-Tal N, Ben-Shaul A, Nicholls A, Honig B. Free-energy determinants of α-helix insertion into lipid bilayers. Biophys J 1996;70:1803–1812.
49. Russell CJ, Thorgeirsson TE, Shin Y-K. Temperature dependence of polypeptide partitioning between water and phospholipid bilayers. Biochemistry 1996;35:9526–9532.
50. Jain MK, Rogers J, Simpson L, Gierash LM. Effect of tryptophan derivatives on the phase properties of bilayers. Biochim Biophys Acta 1985;816:153–162.
51. Seelig J, Ganz P. Nonclassical hydrophobic effect in membrane binding equilibria. Biochemistry 1991;30:9354–9359.
52. Katzer M, Stillwell W. Partitioning of ABA into bilayers of di-saturated phosphatidylcholines as measured by DSC. Biophys J 2003;84:314–325.
53. Wimley WC, White SH. Membrane partitioning: distinguishing bilayer effects from the hydrophobic effect. Biochemistry 1993;32:6307–6312.
54. DeVido DR, Dorsey JG, Chan HS, Dill KA. Oil/water partitioning has a different thermodynamic signature when the oil solvent chains are aligned than when they are amorphous. J Phys Chem B 1998;102:7272–7279.
55. Yau WM, Wimley WC, Gawrisch K, White SH. The preference of tryptophan for membrane interfaces. Biochemistry 1998;37:14713–14718.
56. Wimley WC, White SH. Experimentally determined hydrophobicity scale for proteins at membrane interfaces. Nat Struct Biol 1996;3:842–848.
57. Wimley WC, Gawrisch K, Creamer TP, White SH. A direct measurement of salt-bridge solvation energies using a peptide model system: implications for protein stability. Proc Natl Acad Sci USA 1996;93:2985–2990.
58. Ladokhin AS, Legmann R, Collier RJ, White SH. Reversible refolding of the diphtheria toxin T-domain on lipid membranes. Biochemistry 2004;43:7451–7458.
59. Ladokhin AS, White SH. Interfacial folding and membrane insertion of a designed helical peptide. Biochemistry 2004;43:5782–5791.
60. Dill KA, Chan HS. From Levinthal to pathways to funnels. Nat Struct Biol 1997;4:10–19.
61. Onuchic JN, Nymeyer H, Garcia AE, Chahine J, Socci ND. The energy landscape theory of protein folding: insights into folding mechanisms and scenarios. Adv Protein Chem 2000;53:87–152.
62. Nagle JF, Tristram-Nagle S. Structure of lipid bilayers. Biochim Biophys Acta Rev Biomembr 2000;1469:159–195.
63. Brooks BR, et al. CHARMM: a program for macromolecular energy, minimization, and dynamics calculations. J Comput Chem 1983;4:187–217.
64. Schlenkrish M, Brickmann J, MacKerell AD Jr, Karplus M. Empirical potential energy function for phospholipids: criteria for parameter optimizaton and applications. In: Merz KM, Roux B, editors. Biological membranes: a molecular perspective from computation and experiment. Boston: Birkhaüser; 1996. p 31–81.
65. Feller SE, Yin D, Pastor RW, MacKerell AD Jr. Molecular dynamics simulation of unsaturated lipid bilayers at low hydration: parameterization and comparison with diffraction studies. Biophys J 1997;73:2269–2279.
66. Feller SE, Pastor RW. Constant surface tension simulations of lipid bilayers: the sensitivity of surface areas and compressibilities. J Chem Phys 1999;111:1281–1287.